SAND2015-1044C

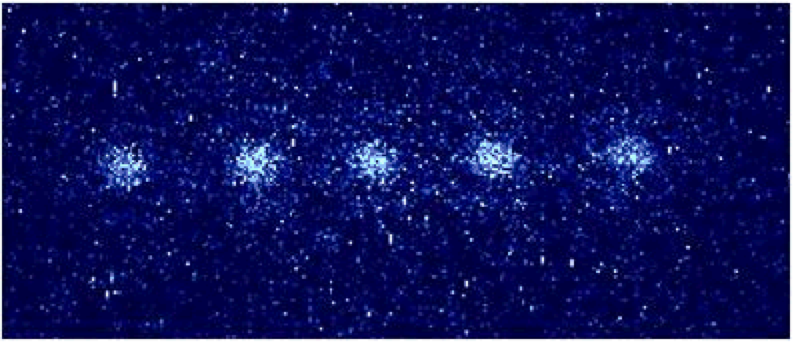

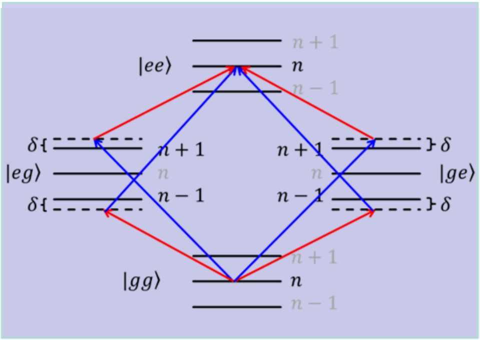

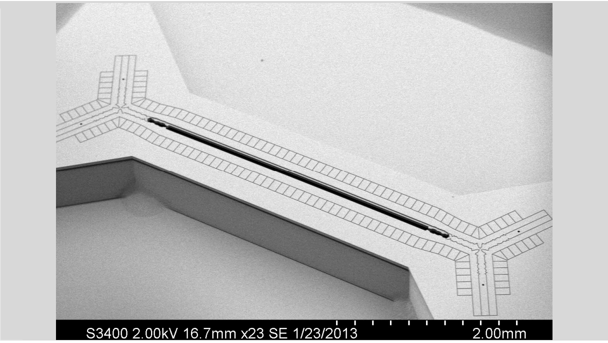

Quantum Information Processing in Sandia surface traps

Peter Maunz, Jonathan Mizrahi, Kenneth Rudinger,
Eric Nielsen, and Robin Blume-Kohout

February, 2015

I A R P A

National Nuclear Security Administration

U.S. DEPARTMENT OF ENERGY

Sandia National Laboratories is a multi-program laboratory managed and operated by Sandia Corporation, a wholly owned subsidiary of Lockheed Martin Corporation, for the U.S. Department of Energy's National Nuclear Security Administration under contract DE-AC04-94AL85000.

Towards scalable ion traps

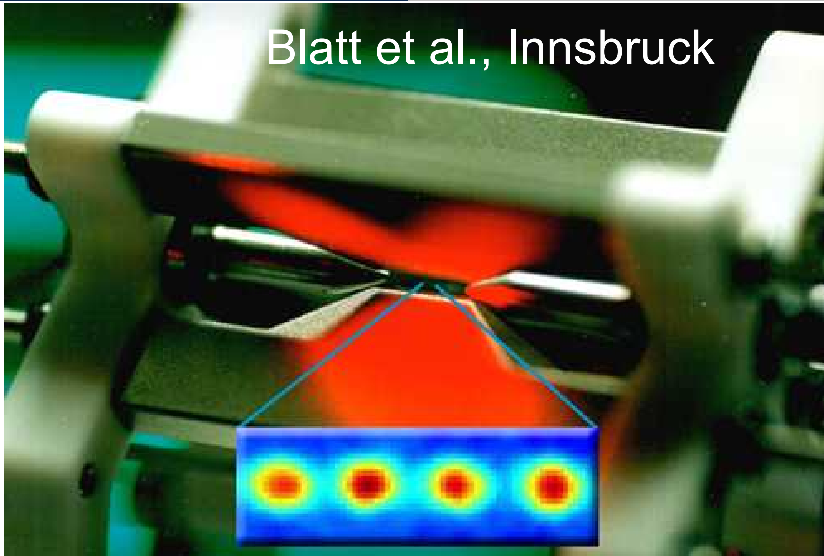

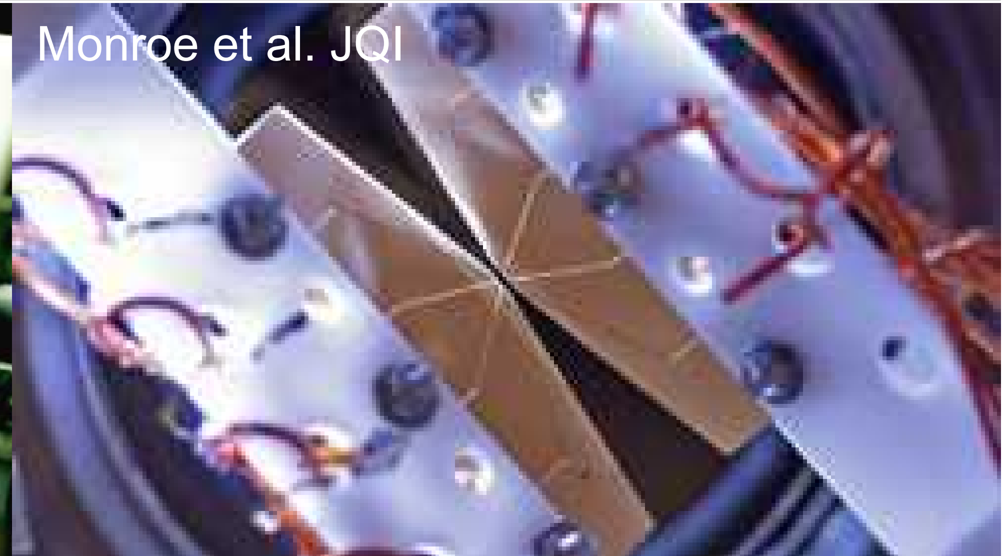

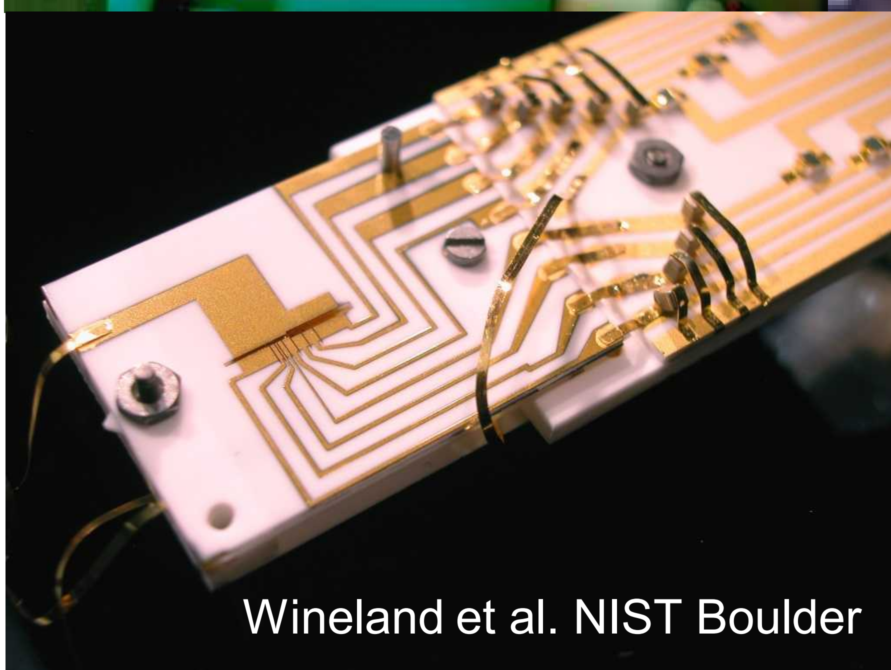

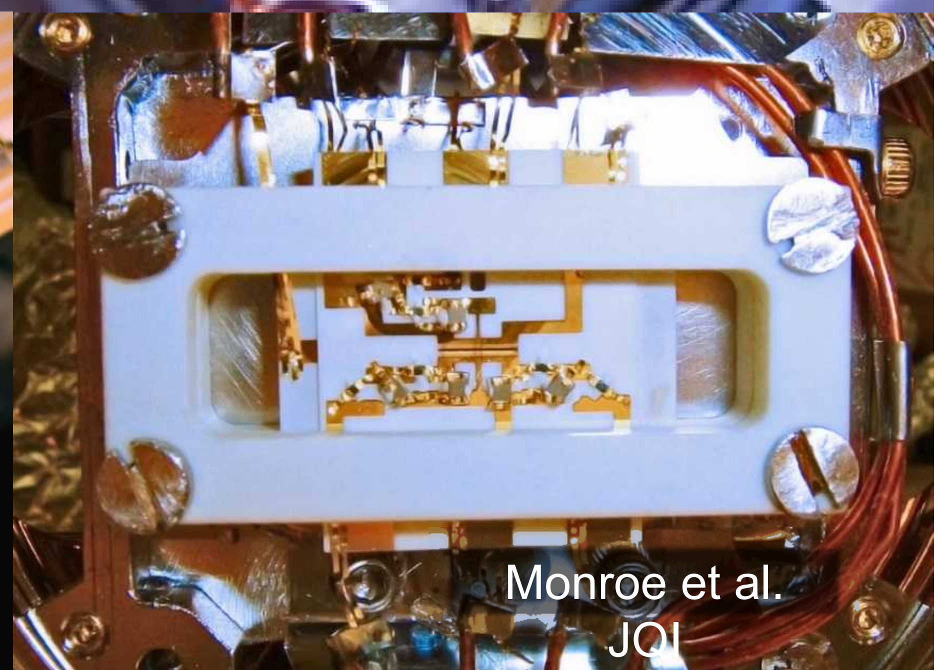

Micro-fabrication

- Microfabrication enables scalable traps
- Optimize traps for Quantum information processing
- In realizing QIP we can learn and solve
  the challenges in small micro-fabricated traps

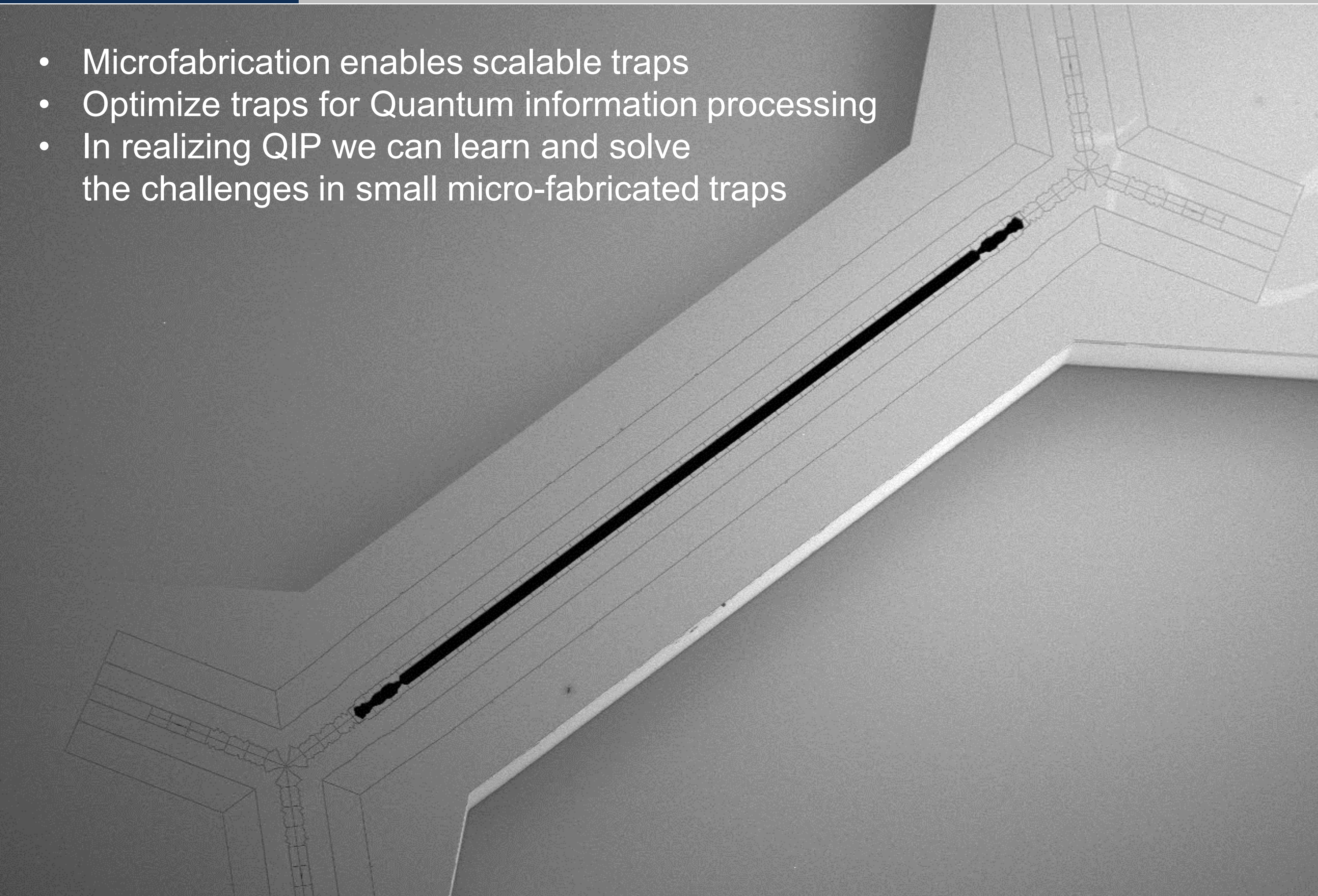

The Ytterbium Qubit

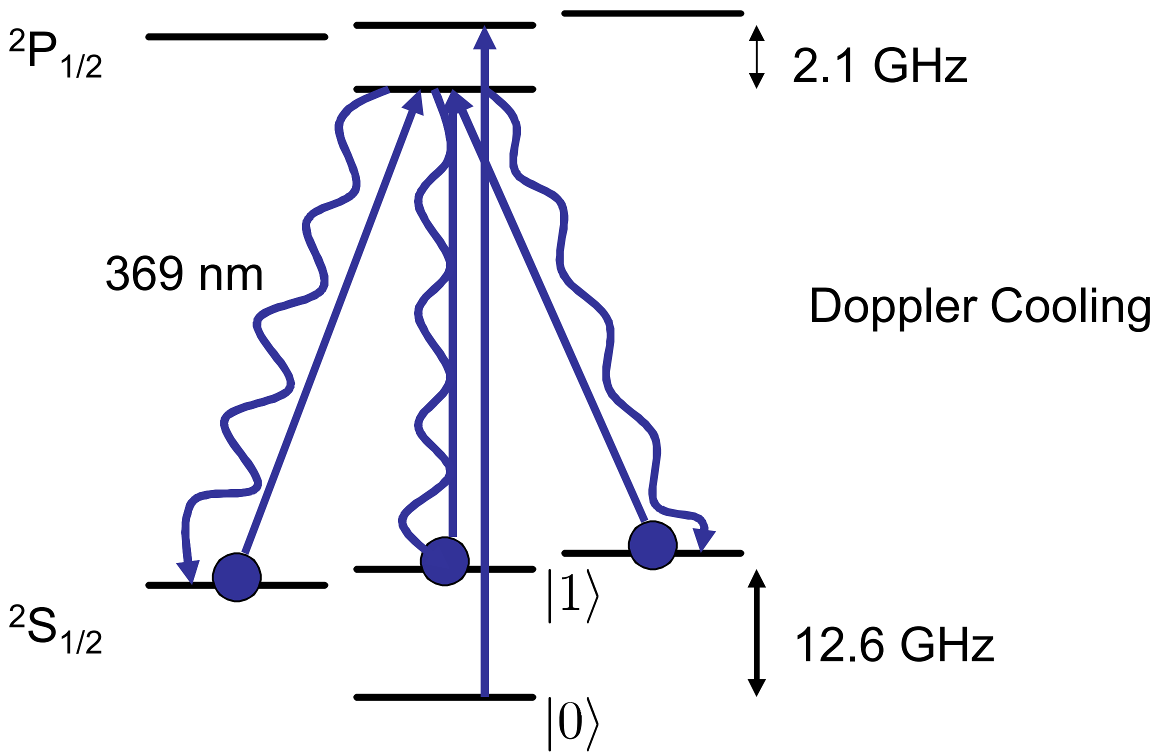

clock state qubit, magnetic field insensitive.

S. Olmschenk *et al.*, PRA **76**, 052314 (2007)

Gate Set Tomography

State and Process Tomography

$$\langle\langle E_k | \quad G_{\text{analyze}} \; G_{\text{characterize}} \; G_{\text{prepare}} \quad |\rho\rangle\rangle$$

$$\langle\langle E_j | G_{\text{characterize}} | \rho_i \rangle\rangle$$

- Needs perfect gates to prepare and analyze
- Often done retrospectively

Gate Set Tomography
(Developed by Robin Blume-Kohout et al.)

- Does not rely on perfect gates, operation of gates is extracted from their operation
- Characterize the gates first, then predict the outcome of a sequence of gates

Robin Blume-Kohout et al. *Robust, Self-consistent, Closed-form Tomography of Quantum Logic Gates on a Trapped Ion Qubit*. ArXiv 1310.4492 e-print, October 16, 2013.

GST: results

	ML estimate (short dataset)	ML estimate (long dataset)	Target gates
ρ	$\begin{pmatrix} 0.0099 & 0.0077-0.0046i \\ h.c. & 0.9901 \end{pmatrix}$	$\begin{pmatrix} 0.0092 & -0.0017+0.0088i \\ h.c. & 0.9908 \end{pmatrix}$	$\begin{pmatrix} 0 & 0 \\ 0 & 1 \end{pmatrix}$
E	$\begin{pmatrix} 0.9911 & 0.0166-0.0006i \\ h.c. & 0.0089 \end{pmatrix}$	$\begin{pmatrix} 0.988 & 0.0019+0.0089i \\ h.c. & 0.012 \end{pmatrix}$	$\begin{pmatrix} 1 & 0 \\ 0 & 0 \end{pmatrix}$
G_1	$\begin{pmatrix} 1.0019 & -0.0128 & -0.0198 & -0.0002 \\ -0.0066 & 0.9775 & -0.0118 & 0.0122 \\ 0.0041 & 0.0842 & 1.0138 & 0.0073 \\ -0.0035 & -0.013 & 0.0075 & 0.9969 \end{pmatrix}$	$\begin{pmatrix} 1.0001 & -0 & 0.0003 & 0.0001 \\ 0.0001 & 0.9994 & -0.0003 & -0 \\ -0.0001 & 0.0006 & 0.999 & -0.0003 \\ -0 & -0.0001 & 0.0002 & 0.9998 \end{pmatrix}$	$\begin{pmatrix} 1 & 0 & 0 & 0 \\ 0 & 1 & 0 & 0 \\ 0 & 0 & 1 & 0 \\ 0 & 0 & 0 & 1 \end{pmatrix}$
G_2	$\begin{pmatrix} 1.0017 & -0.0276 & -0.0276 & -0.0048 \\ -0.0193 & 0.9582 & -0.0076 & -0.0127 \\ -0.0134 & 0.043 & 0.0082 & -0.9987 \\ -0.0072 & 0.002 & 1.0069 & 0.0192 \end{pmatrix}$	$\begin{pmatrix} 1 & -0.0001 & -0.0045 & -0.0005 \\ 0 & 0.9994 & -0.006 & -0.0018 \\ -0.005 & -0.0112 & -0.0064 & -0.9991 \\ 0.0006 & 0.0063 & 0.9993 & 0.0143 \end{pmatrix}$	$\begin{pmatrix} 1 & 0 & 0 & 0 \\ 0 & 1 & 0 & 0 \\ 0 & 0 & 0 & -1 \\ 0 & 0 & 1 & 0 \end{pmatrix}$
G_3	$\begin{pmatrix} 0.99 & -0.0114 & 0.0083 & 0.0044 \\ -0.0082 & -0.0141 & -0.0045 & 0.9892 \\ 0.0121 & -0.0044 & 1.0056 & -0.0059 \\ -0.0001 & -0.9848 & 0.0017 & -0.0016 \end{pmatrix}$	$\begin{pmatrix} 1.0001 & 0.0033 & 0.0001 & 0.0049 \\ 0.0033 & -0.0001 & -0.0005 & 0.9992 \\ -0.0002 & -0.0024 & 0.9995 & -0.0161 \\ -0.0019 & -0.9989 & 0.0179 & 0.0085 \end{pmatrix}$	$\begin{pmatrix} 1 & 0 & 0 & 0 \\ 0 & 0 & 0 & 1 \\ 0 & 0 & 1 & 0 \\ 0 & -1 & 0 & 0 \end{pmatrix}$
G_4	$\begin{pmatrix} 0.9983 & -0.0217 & 0.0127 & 0.0142 \\ -0.0039 & 0.9745 & 0.0034 & 0.0077 \\ -0.0004 & -0.0145 & -1.0473 & -0.0323 \\ -0.014 & -0.0167 & -0.0072 & -1.0024 \end{pmatrix}$	$\begin{pmatrix} 1.0001 & -0 & 0.0062 & 0.0028 \\ -0 & 0.9997 & 0.0127 & 0.0022 \\ 0.0066 & 0.0164 & -0.9976 & 0.0065 \\ -0.004 & -0.0004 & -0.0066 & -0.9981 \end{pmatrix}$	$\begin{pmatrix} 1 & 0 & 0 & 0 \\ 0 & 1 & 0 & 0 \\ 0 & 0 & -1 & 0 \\ 0 & 0 & 0 & -1 \end{pmatrix}$

GST: non-Markovian noise

Hierarchical χ^2 for best fit to L=1,2,4,8,16,32

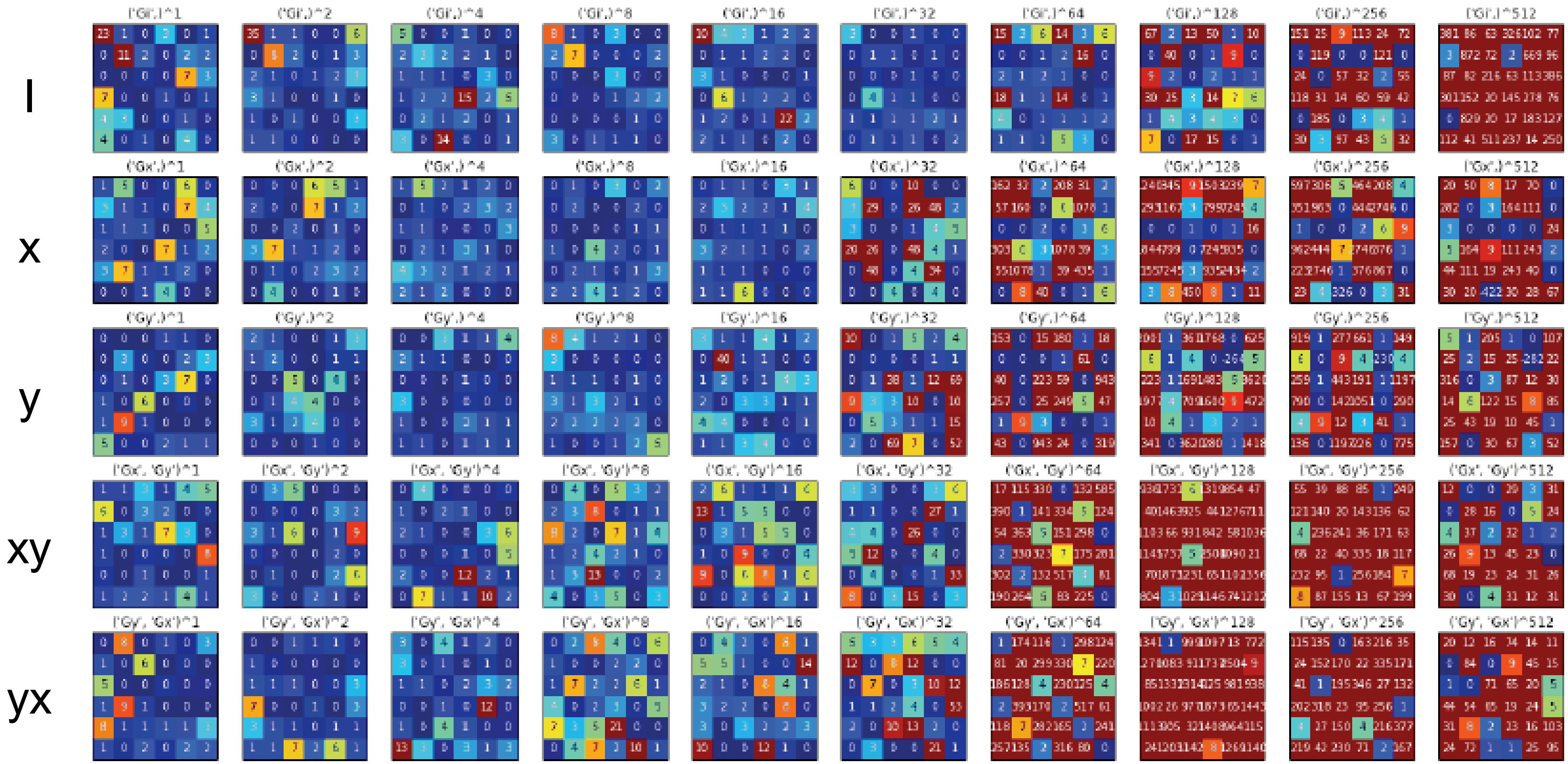

Drift control

- Improved the system: temperature stabilization, elimination of components from microwave system
- Microwave π-times are measured independently and concurrently
- Feedback (locking) scheme adjusts π-times dynamically

Measured π/2-times

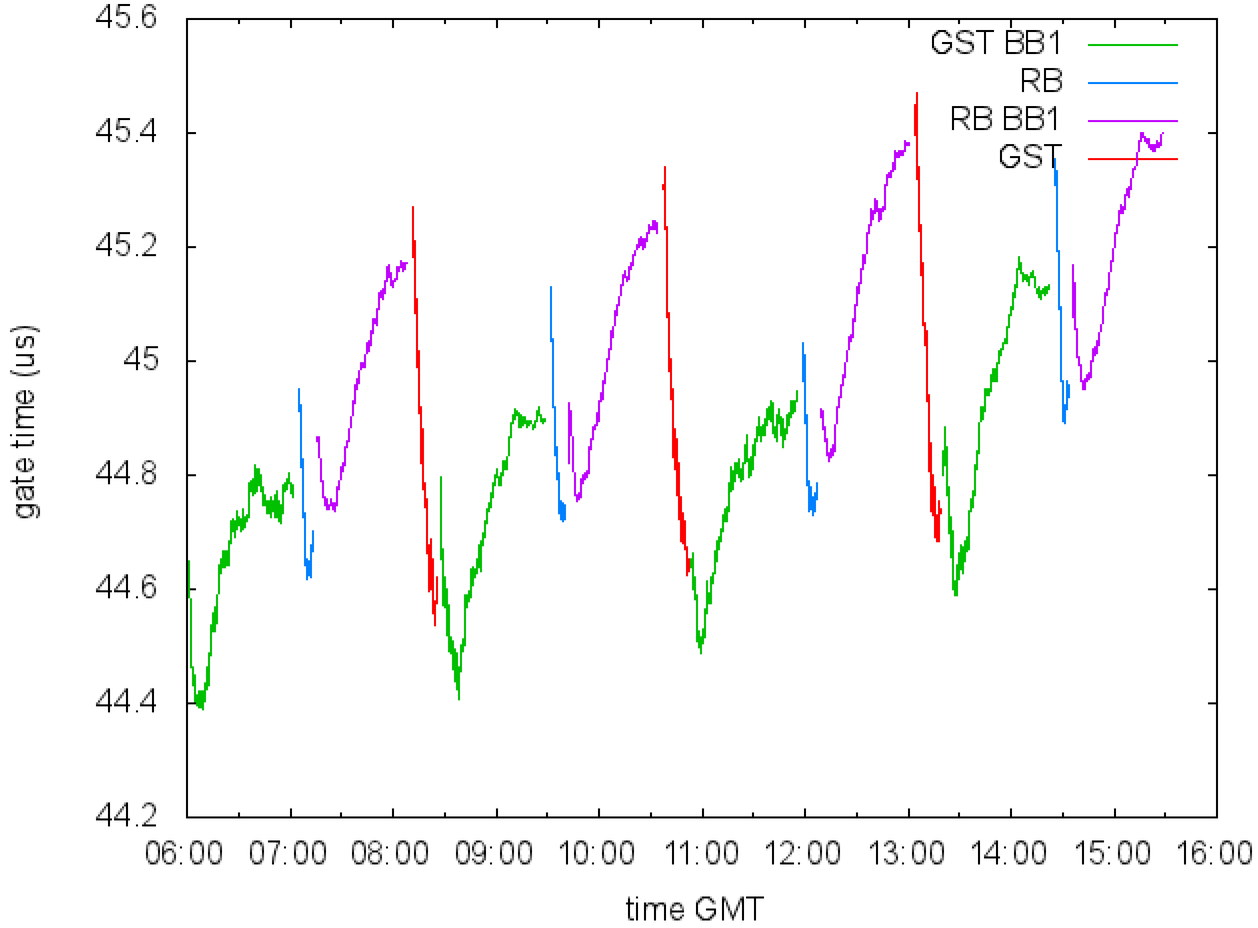

Drift control algorithm

```
GateTimeIntegrator = GateTime << 5

GST sequence

Prepare dark state
Apply 21 GateTime microwave pulse
State detection result = 1 if bright else 0

GateTimeIntegrator -= result
GateTime = GateTimeIntegrator >> 5
```

GST: results

Realized gates

Gate	Matrix (Pauli basis)			
Gi	1.0	0	0	0
	0	1.0	−0.004	0.001
	0	0.009	0.998	−0.038
	0	0.001	0.037	0.992
Gx	1.0	0	0.005	0.003
	0	1.0	0	−0.003
	0.005	0.001	−0.001	−0.999
	−0.002	0.002	0.999	−0.003
Gy	1.0	−0.002	0	0
	−0.002	0	−0.004	1.0
	0	−0.003	1.0	−0.001
	0	−1.0	0.001	−0.005

Comparison to target gates

Gate	Fidelity	Trace Dist.	Frobenius Dist.	Error Generator			
Gi	0.997424	0.054254	0.020661	0	0	0	0
				0	0	−0.004	0.001
				0	0.009	−0.001	−0.038
				0	0.001	0.037	−0.007
Gx	0.999653	0.00939	0.003764	0	0	0.005	0.003
				0	0	0	−0.003
				−0.002	0.002	−0.001	−0.003
				−0.005	−0.001	0.001	−0.001
Gy	0.999944	0.007907	0.003186	0	−0.002	0	0
				0	0	−0.001	0.005
				0	−0.003	0	−0.001
				−0.002	0	−0.004	0

GST results

Gate analysis

Gate	Eigenvalues	Fixed pt	Rotn. axis	Angle	Diag. decay	Off-diag. decay
Gi	$0.996e^{i0.0}$ $0.996e^{-i0.0}$ 1.0 1.0	1.0 0 0.004 0.001	0 0.973 0.017 0.229	0.012037π	0	0.004433
Gx	$0.999e^{i1.6}$ $0.999e^{-i1.6}$ 1.0 1.0	-0.98 0.198 -0.004 -0.001	-0.194 -0.981 0 -0.002	0.500574π	0	0.000625
Gy	$1.0e^{i1.6}$ $1.0e^{-i1.6}$ 1.0 1.0	1.0 0 -0.558 0	-0.299 0.002 -0.954 -0.003	0.500854π	0	0

non-Markovian noise after optimization

χ^2 of GST fit (BB1 compensated microwave gates)

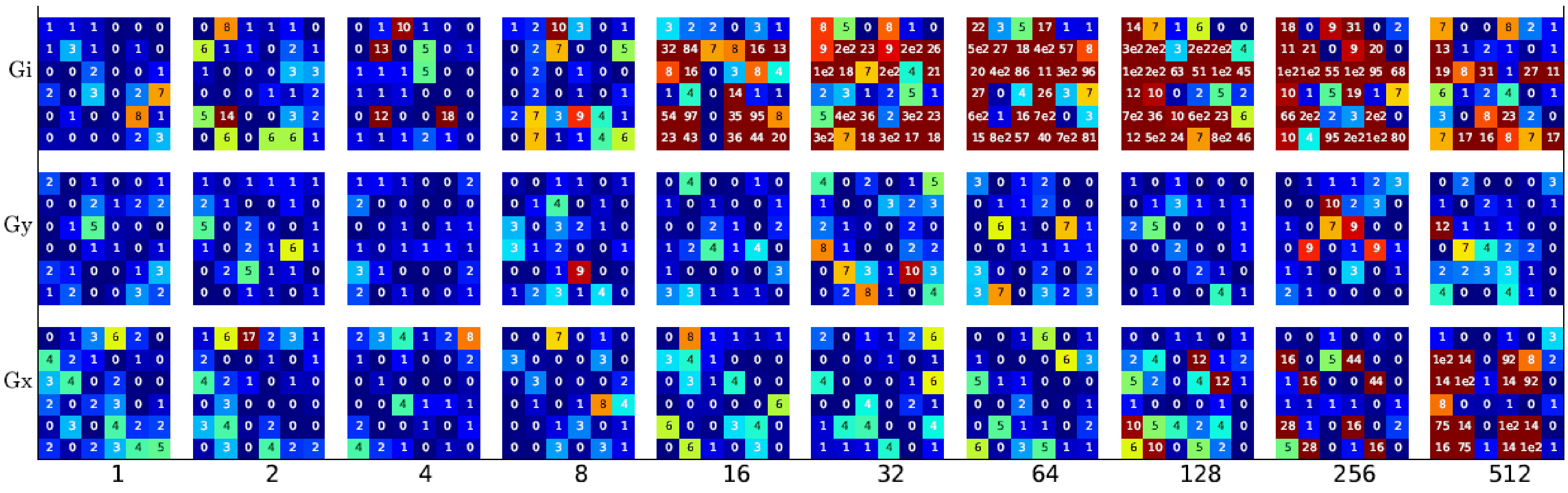

- Very good results for the BB1 compensated gates Gx and Gy
- Programming error in compensation of Gi leads to non-Markovian noise

Randomized benchmarking and GST

Randomized Benchmarking:

- Average infidelity per gate 4.9×10^{-5}
- GST worst case gate infidelity 3×10^{-3}

Randomized benchmarking
Experimental

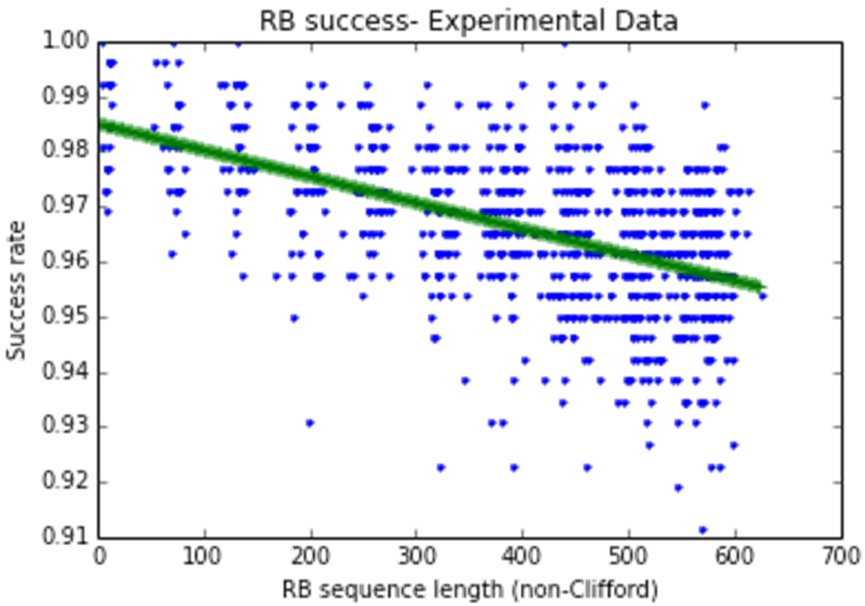

Randomized benchmarking
Markovianized simulated date from GST

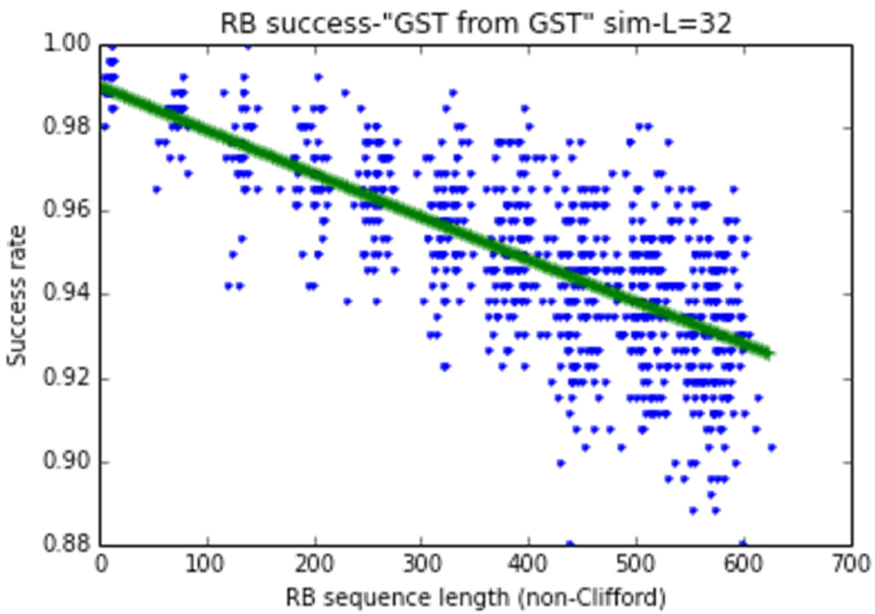

non-Markovian errors average out in Randomized benchmarking

355 Raman transitions: $^{171}Yb^{+}$

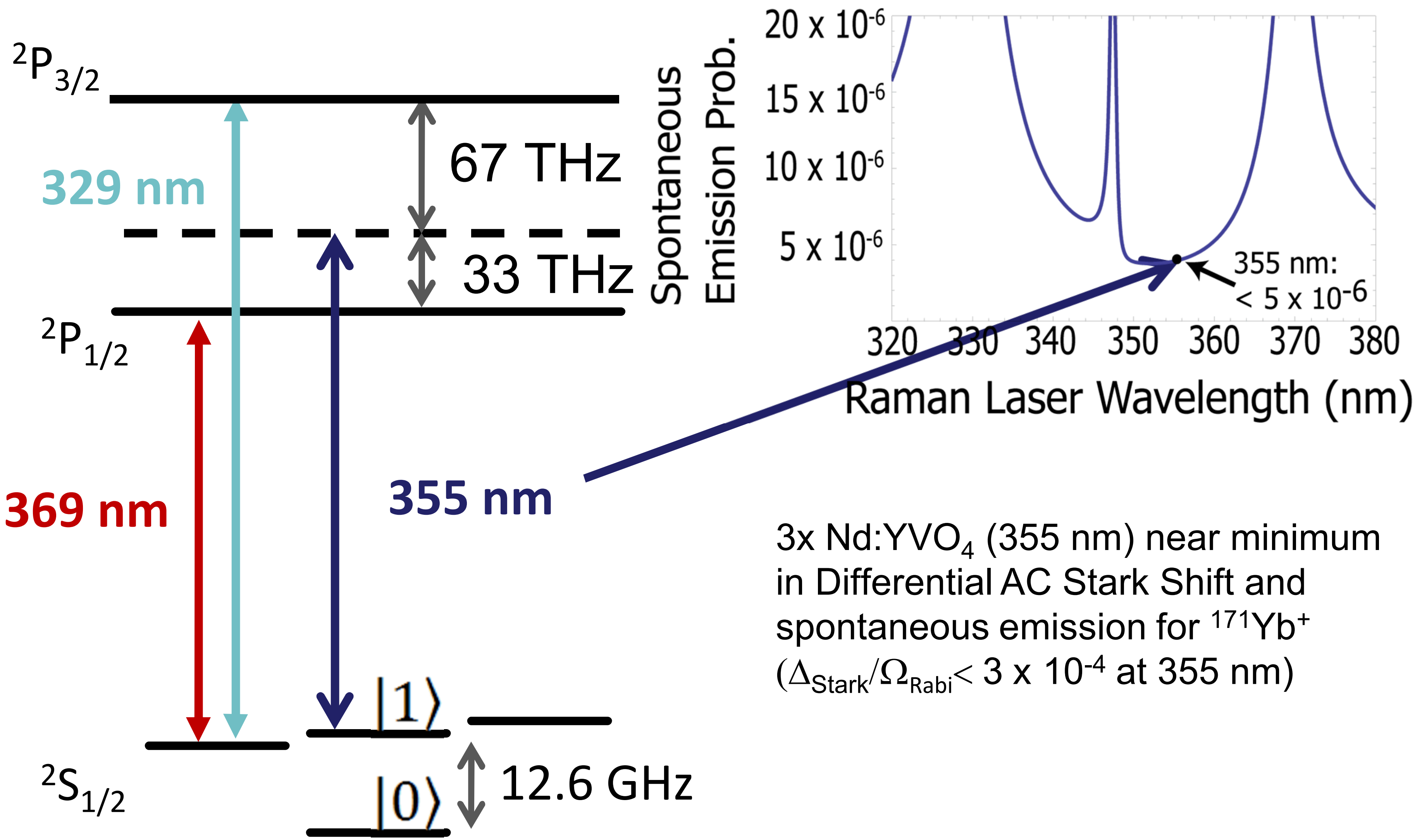

3x $Nd:YVO_4$ (355 nm) near minimum in Differential AC Stark Shift and spontaneous emission for $^{171}Yb^{+}$ ($\Delta_{Stark}/\Omega_{Rabi} < 3 \times 10^{-4}$ at 355 nm)

Pulsed laser Raman transitions

- Couple to ions using 355nm frequency comb
- Beat note created by repetition rate and AOM shift
- Get large splitting for free

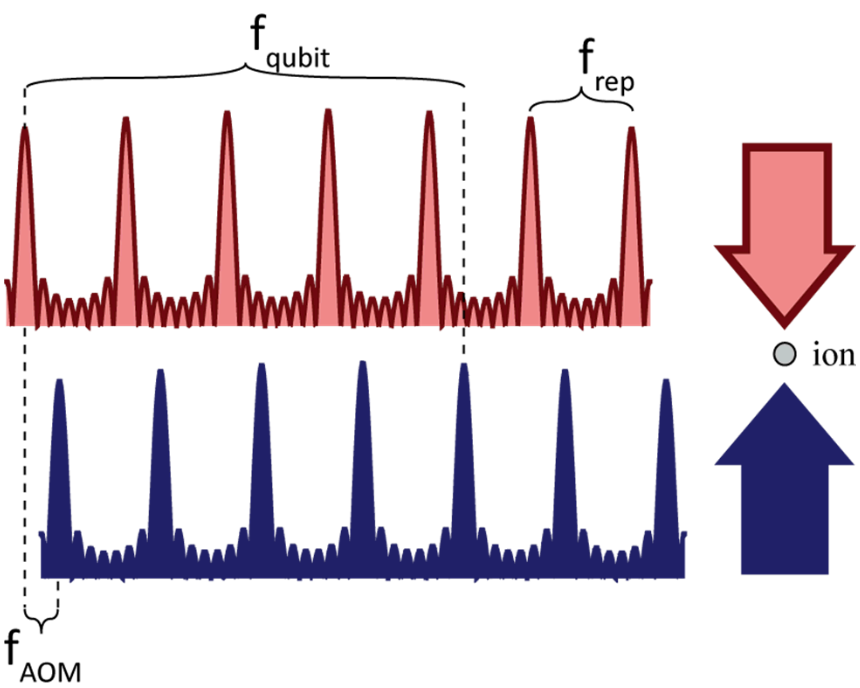

Requirement:

$$f_{qubit} = nf_{rep} \pm f_{AOM}$$

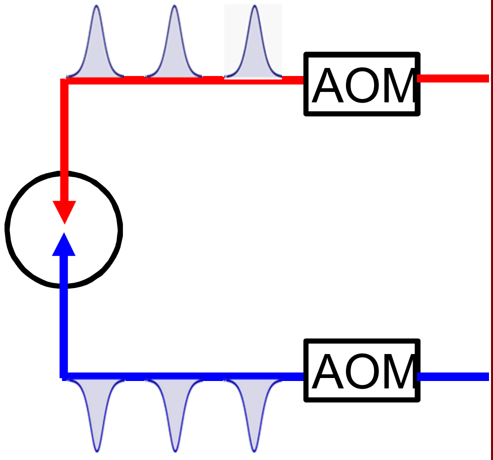

Pulsed laser Raman transitions

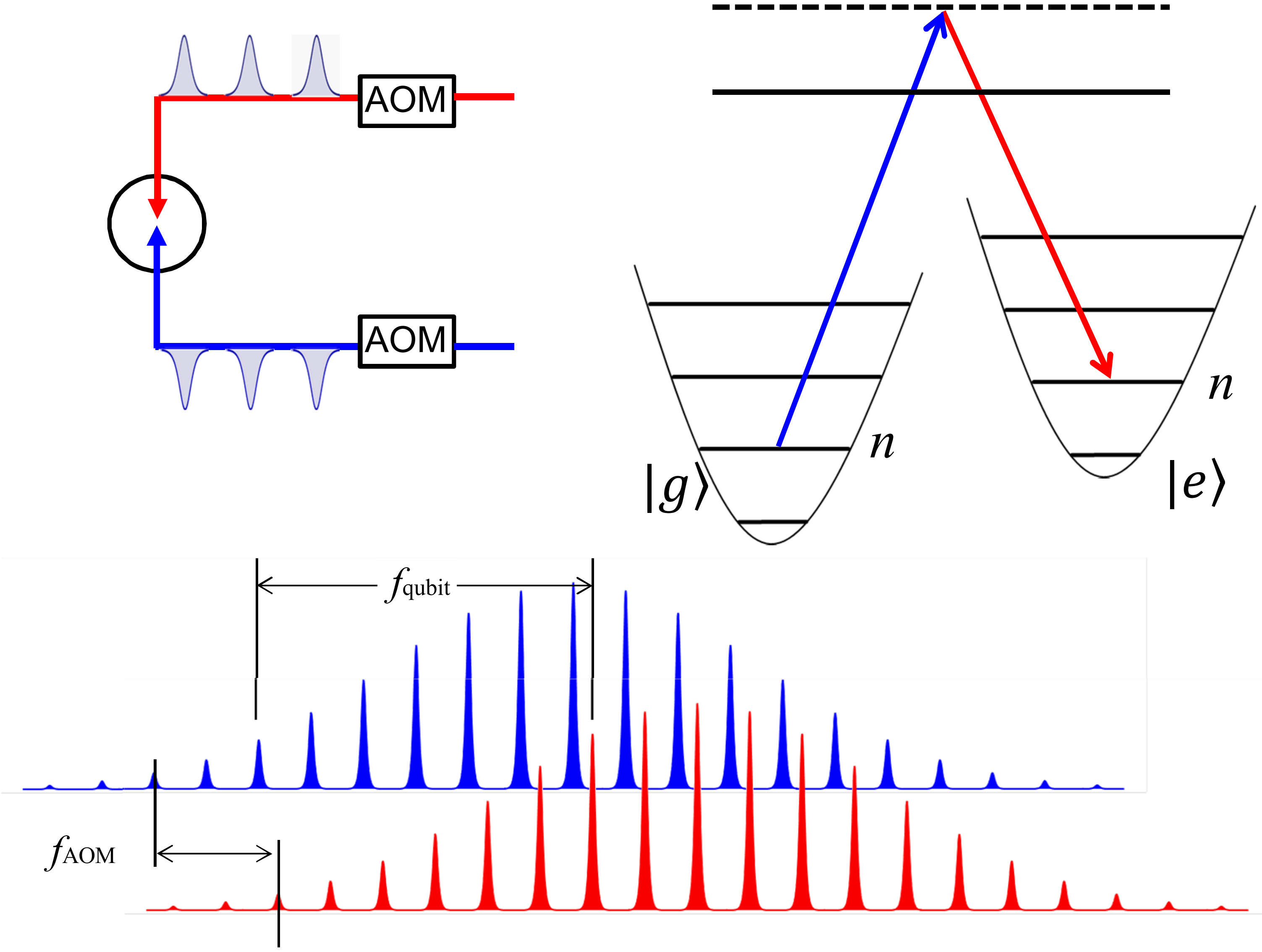

Pulsed laser Raman transitions

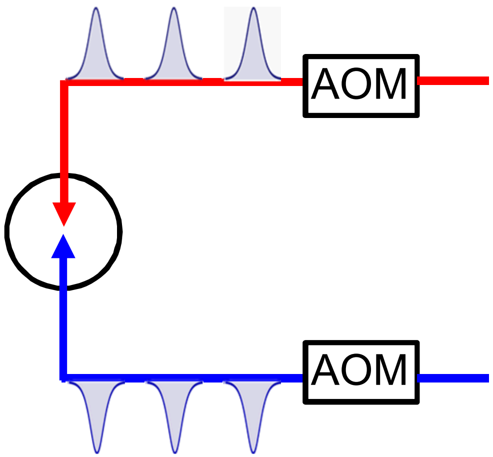

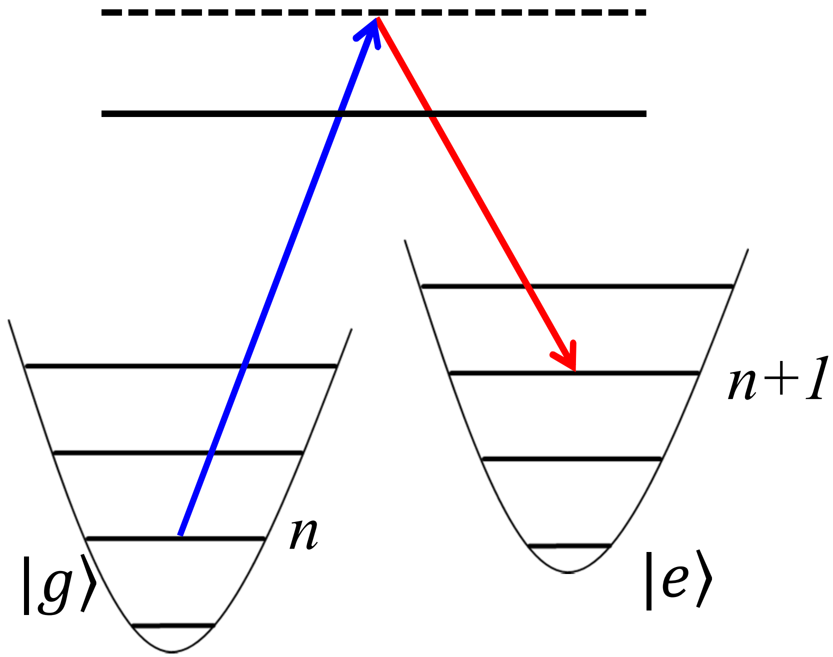

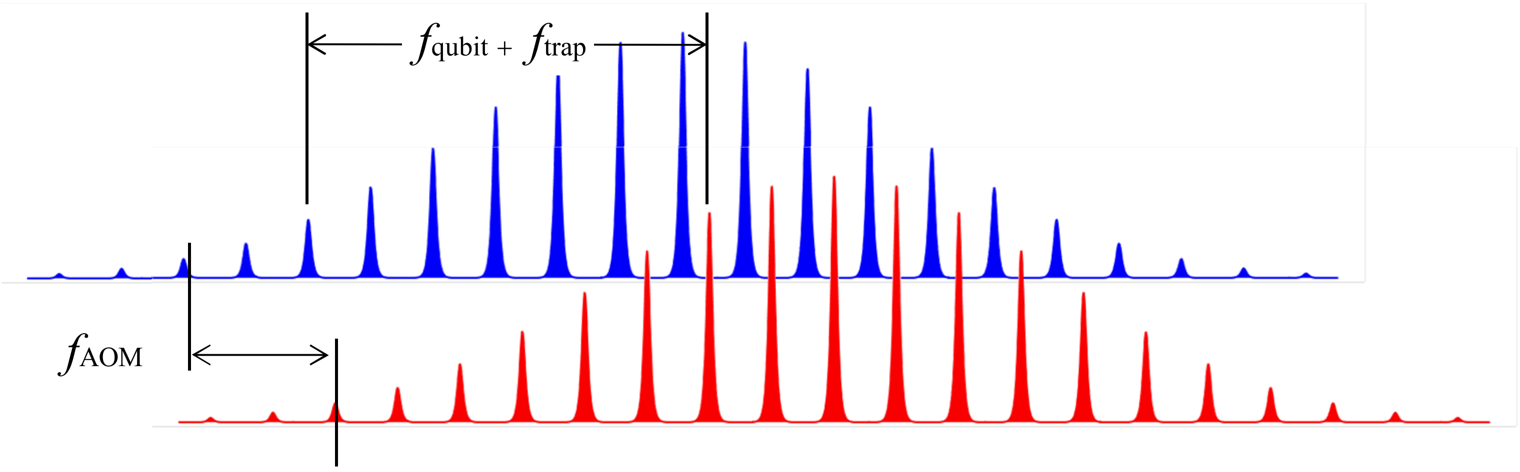

Pulsed laser Raman transitions

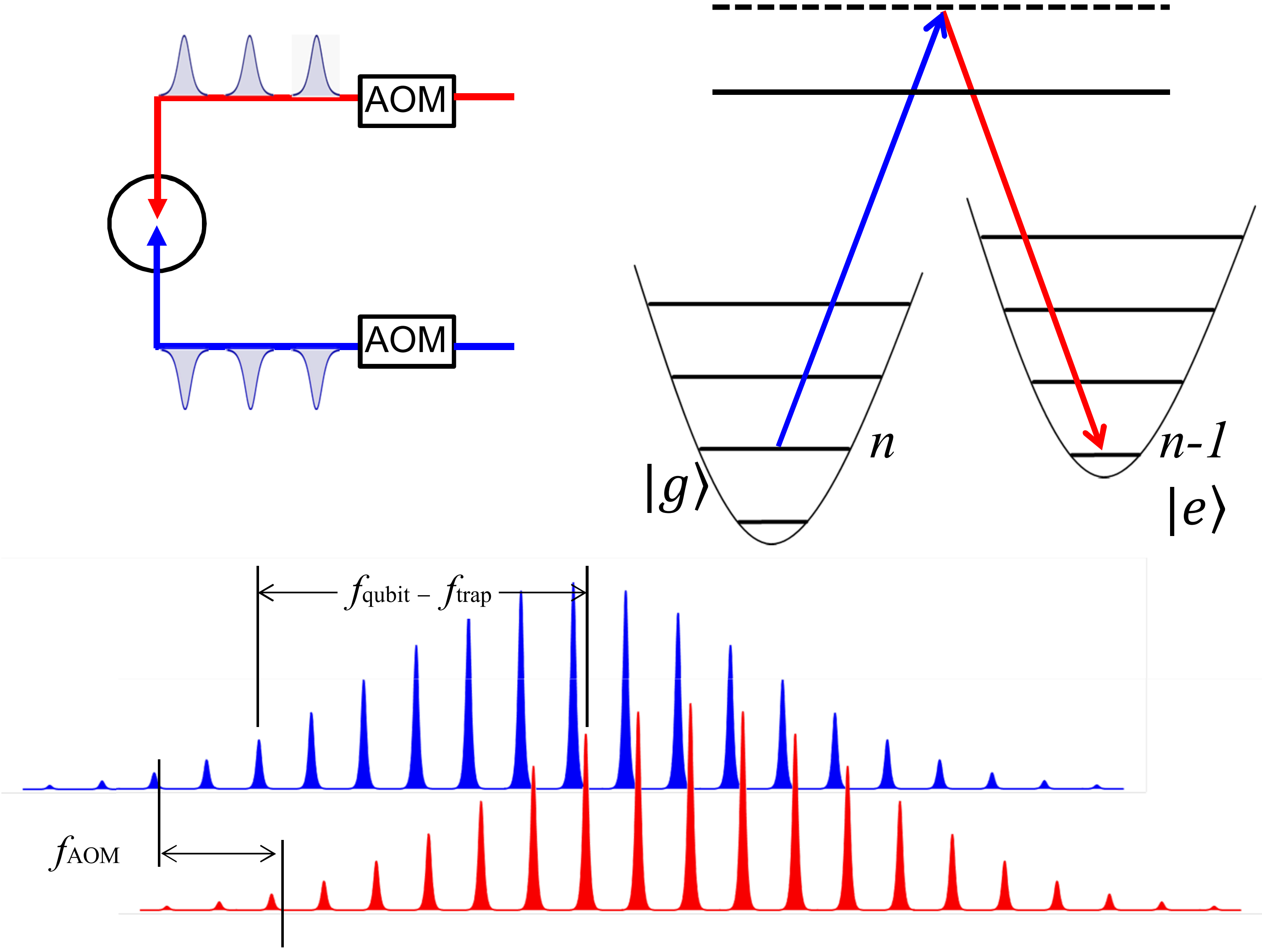

Coherence time

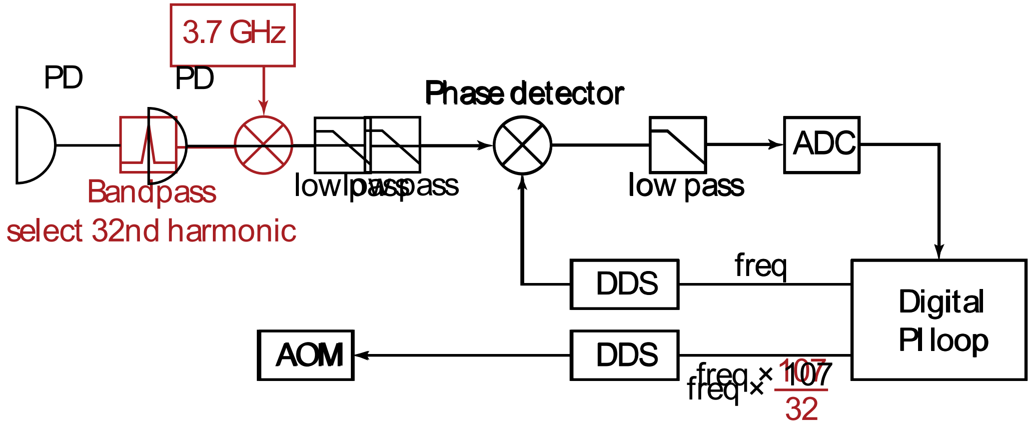

Lock at fundamental:

- 85% contrast between 100μs and 1s

Lock at 32nd harmonic

- Coherence time > 2s

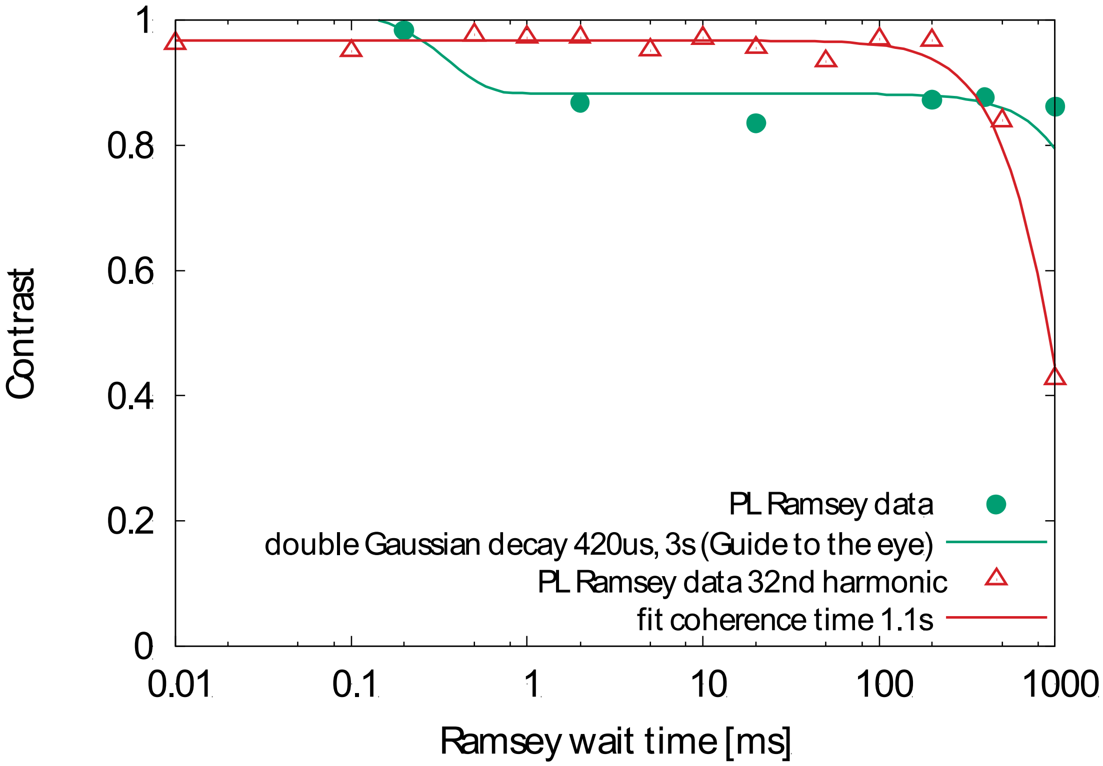

Sideband cooling

- Ground state cooling evident when red sideband cannot be driven
- Data shows ground state cooling of two ion radial tilt mode, $\bar{n} \ll 1$

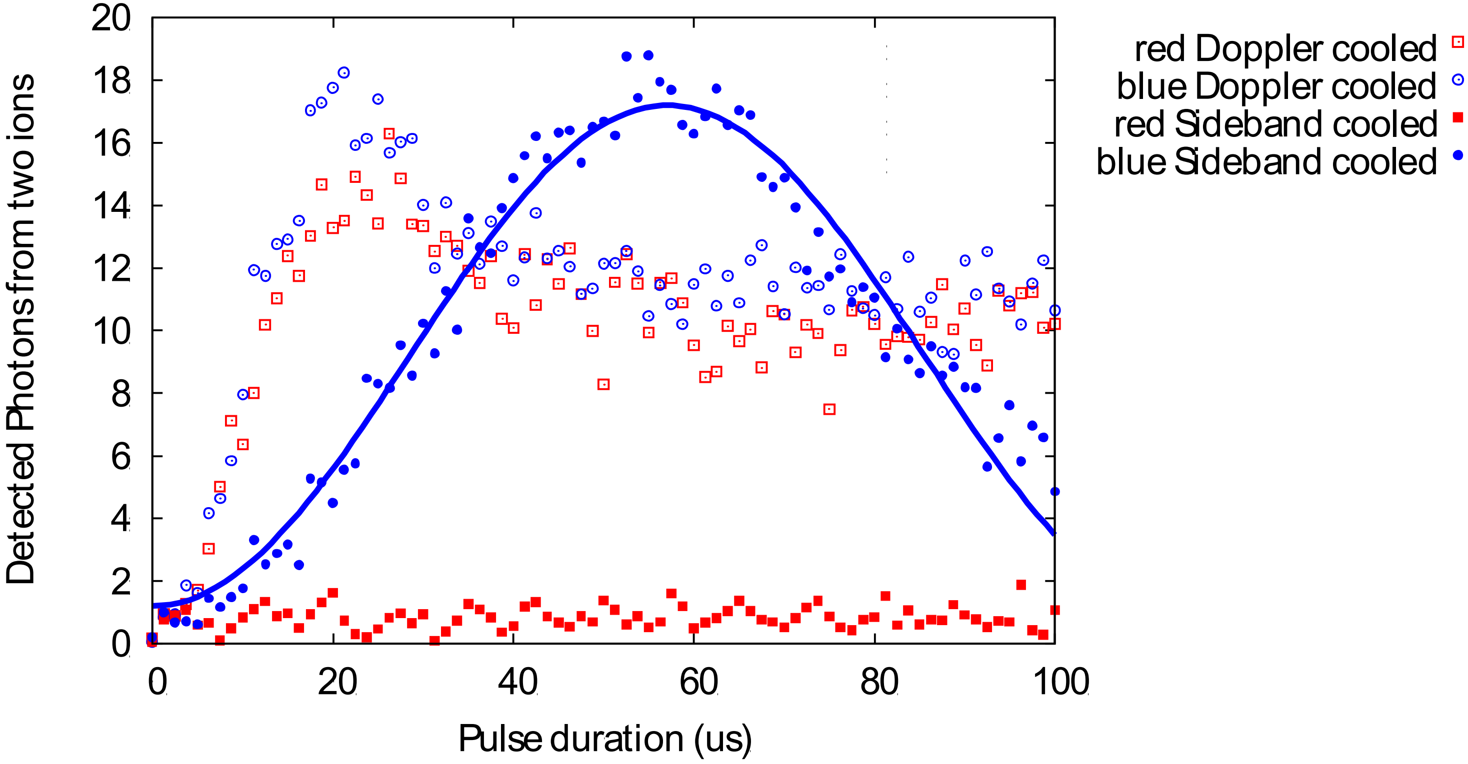

Heating in Two Ion Chain

Transversal Center of Mass

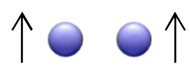

2 modes

Transversal Tilt

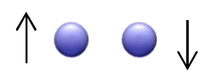

2 modes

Longitudinal Center of Mass

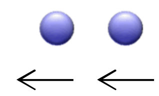

Longitudinal Stretch

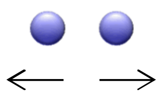

1.94 MHz CoM

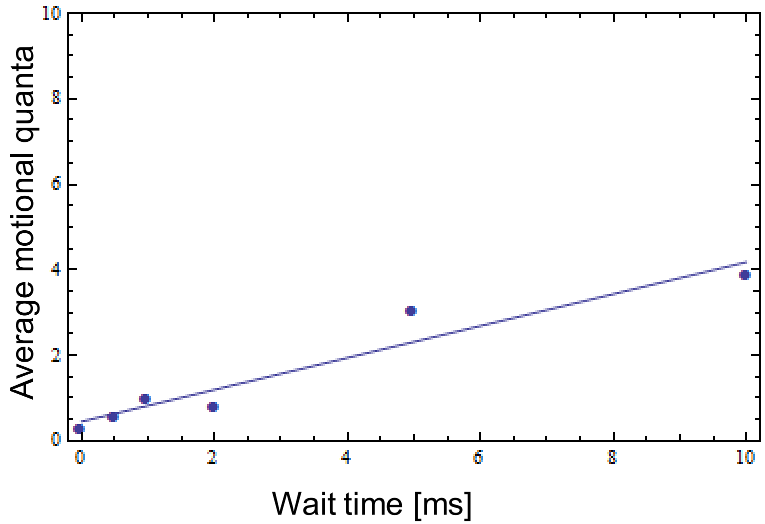

Fit: 0.4 quanta/ms

2.38 MHz CoM

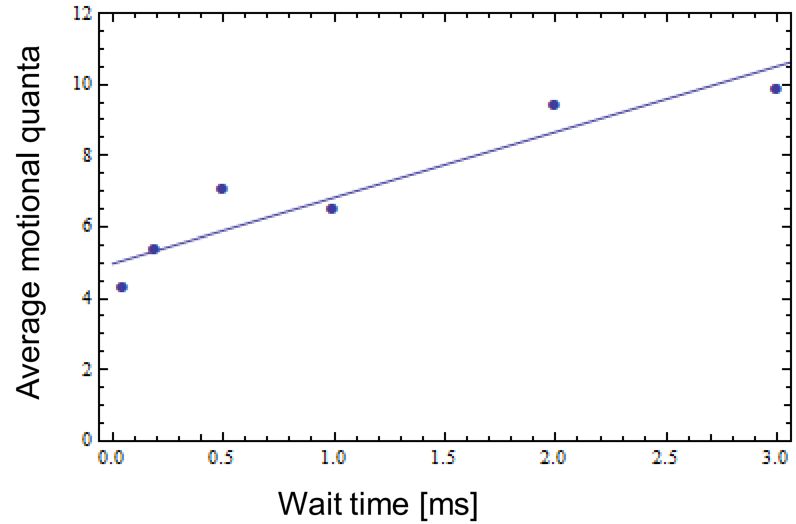

Fit: 1.8 quanta/ms

- Reduced heating to 0.3 q/ms and 1 q/ms when using battery instead of DAC
- Currently limited by technical noise, improvements on the way

Heating in Two Ion Chain

1.84 MHz tilt

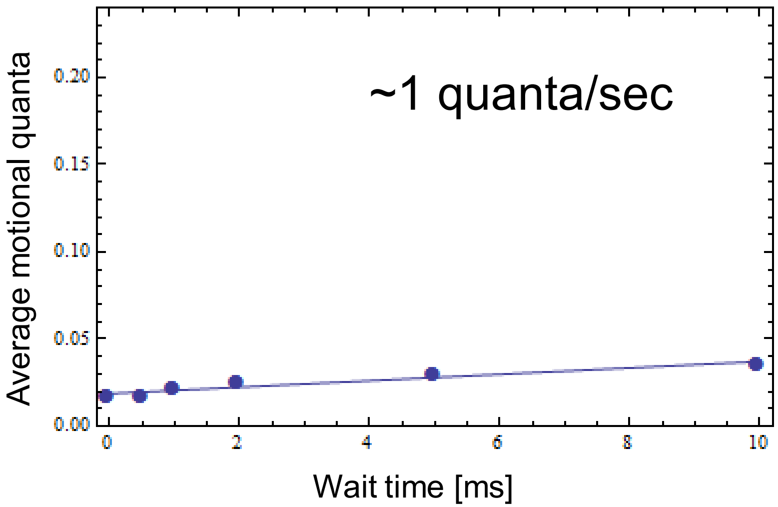

2.32 MHz tilt

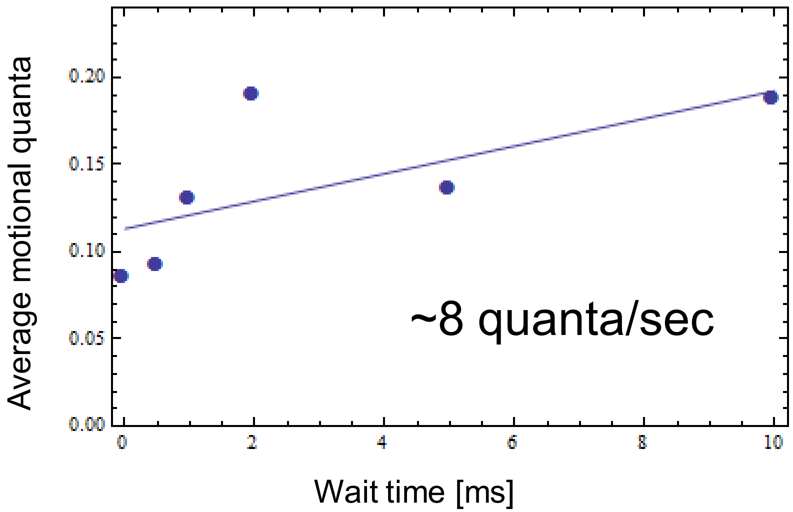

- Using tilt mode near 1.84 MHz for gate
- Lowest heating <1 quanta/sec

Entangling Gate

Basic idea: Use common motion of the ions to mediate entanglement

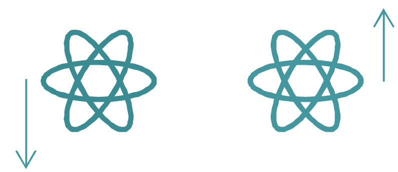

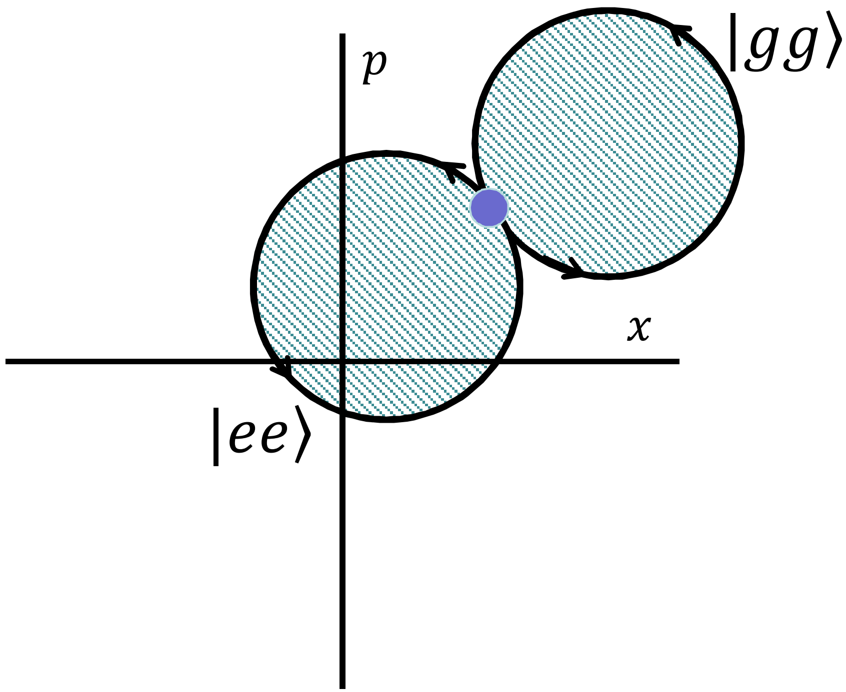

- Raman beams create *spin-dependent force*
- Force drives the ions away from and then back to their starting position

- Spin dependent phase remains

[1] K. Mølmer, A. Sørensen, PRL 82, 1835 (1999)
[2] A. Sørensen, K. Mølmer, PRL 82, 1971 (1999)
[3] A. Sørensen, K. Mølmer, PRA 62, 022311 (2000)

Entangling Gate

Creating a spin-dependent force with Raman beams:
Apply red and blue detuned sidebands simultaneously

$$\omega_{red} = \omega_0 - \nu - \delta$$
$$\omega_{blue} = \omega_0 + \nu + \delta$$

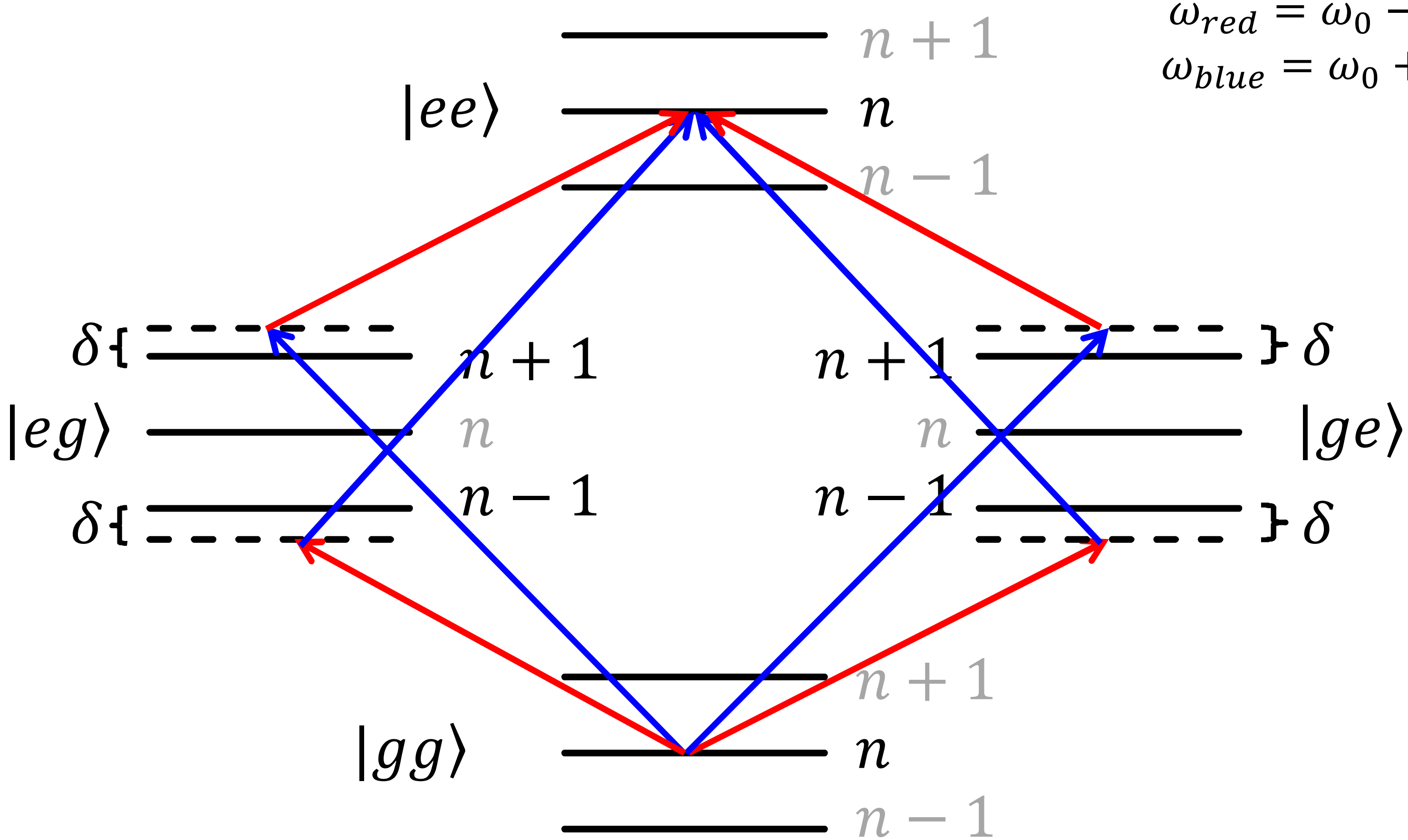

Entangling Gate

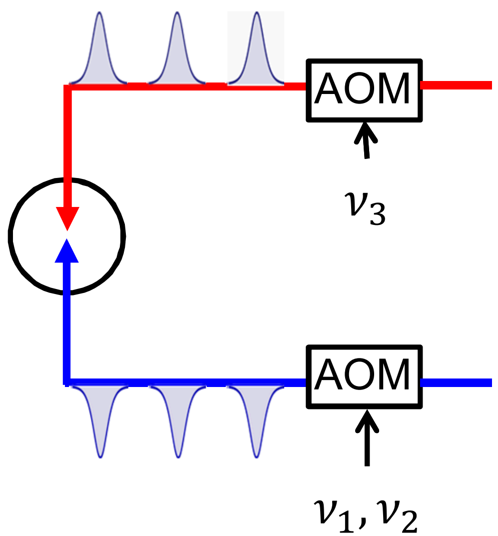

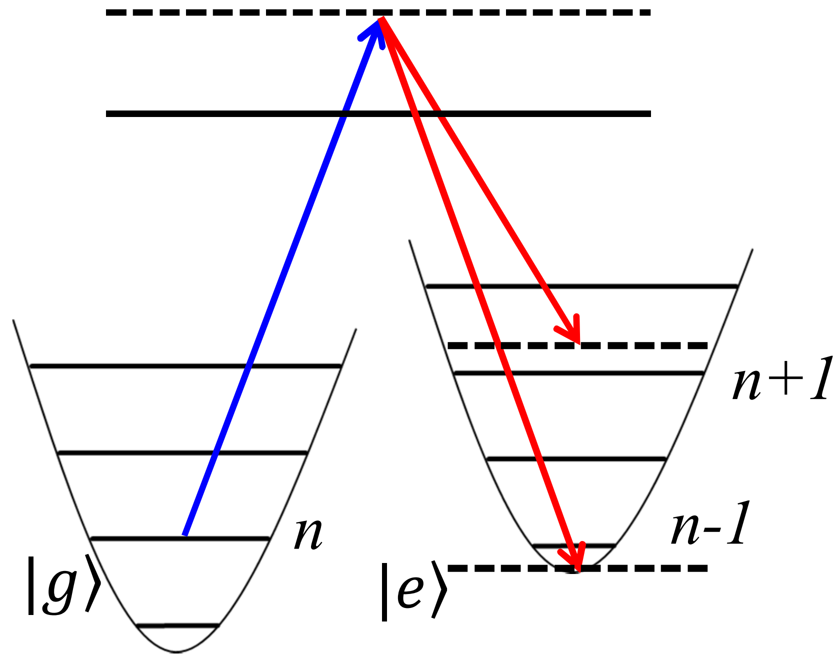

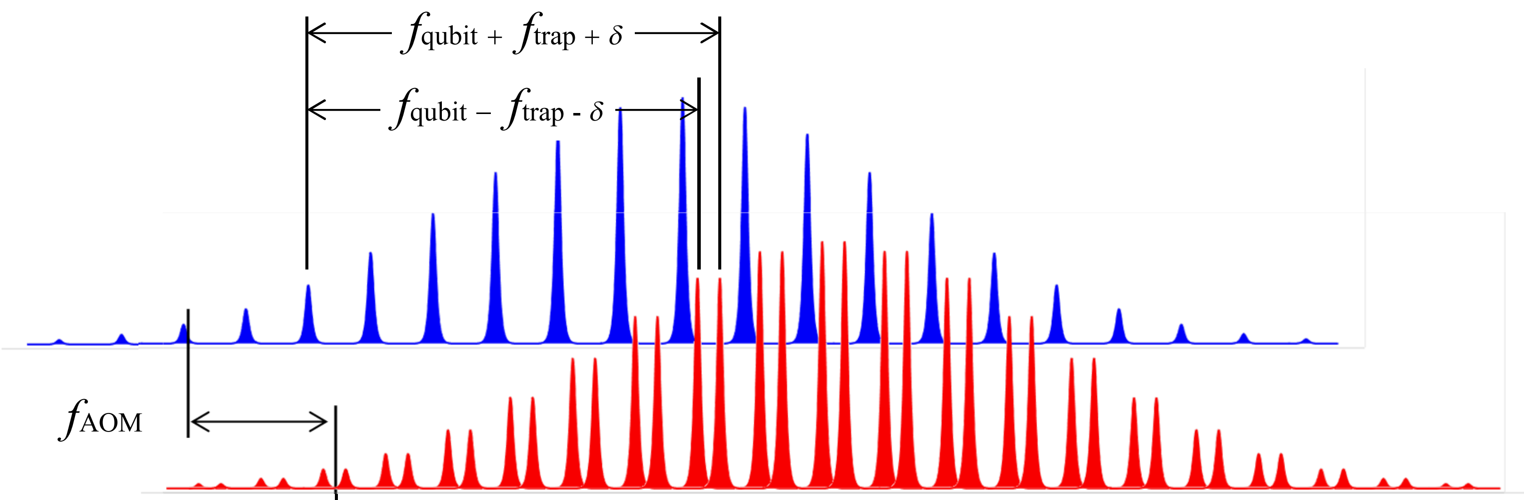

Sandia National Laboratories

Entangling Gate

- Scanning detuning reveals point where gate is optimal

Probability

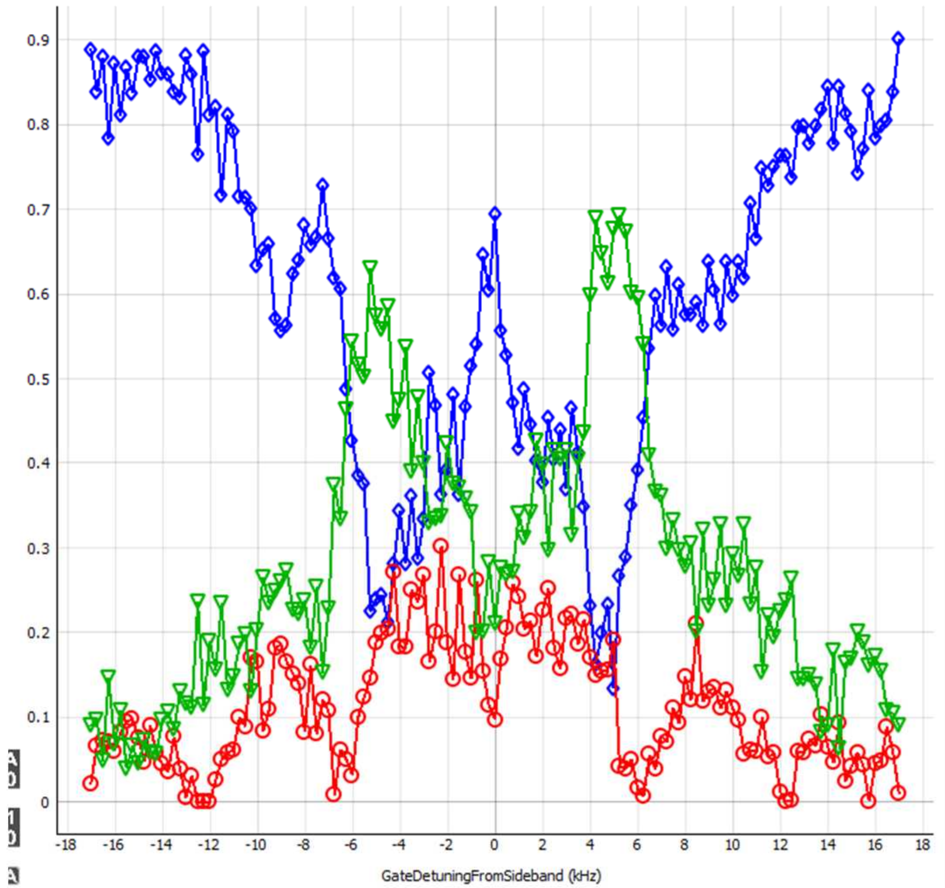

Detuning from sideband (kHz)

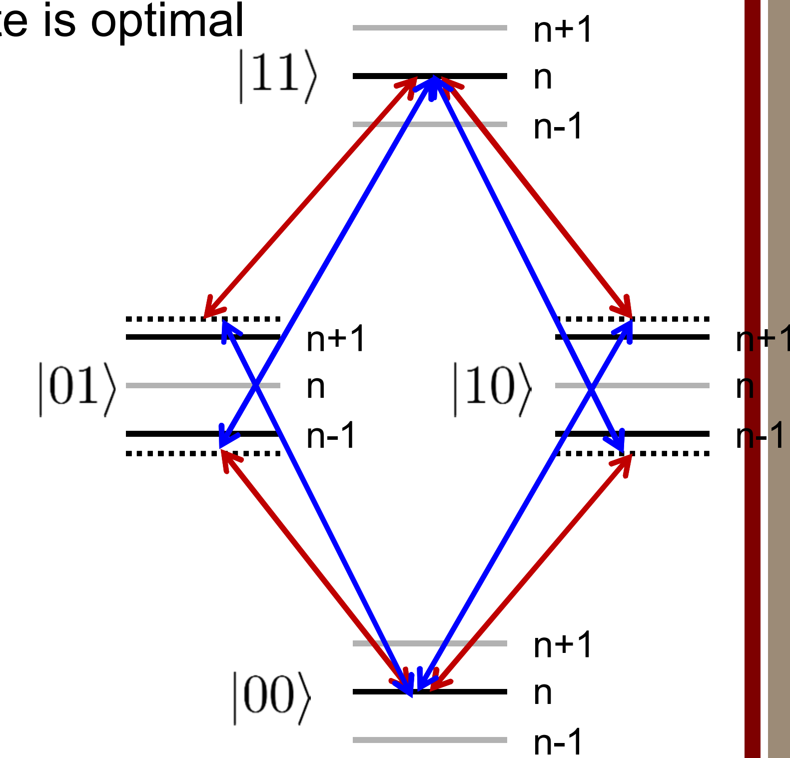

$$|00\rangle \rightarrow |00\rangle + |11\rangle$$

Blue: Zero ions bright

Red: One ion bright

Green: Two ions bright

Entangling Gate – preliminary results

- Populations reveal diagonals of density matrix, parity scan reveals coherences
- Taken together they yield the fidelity

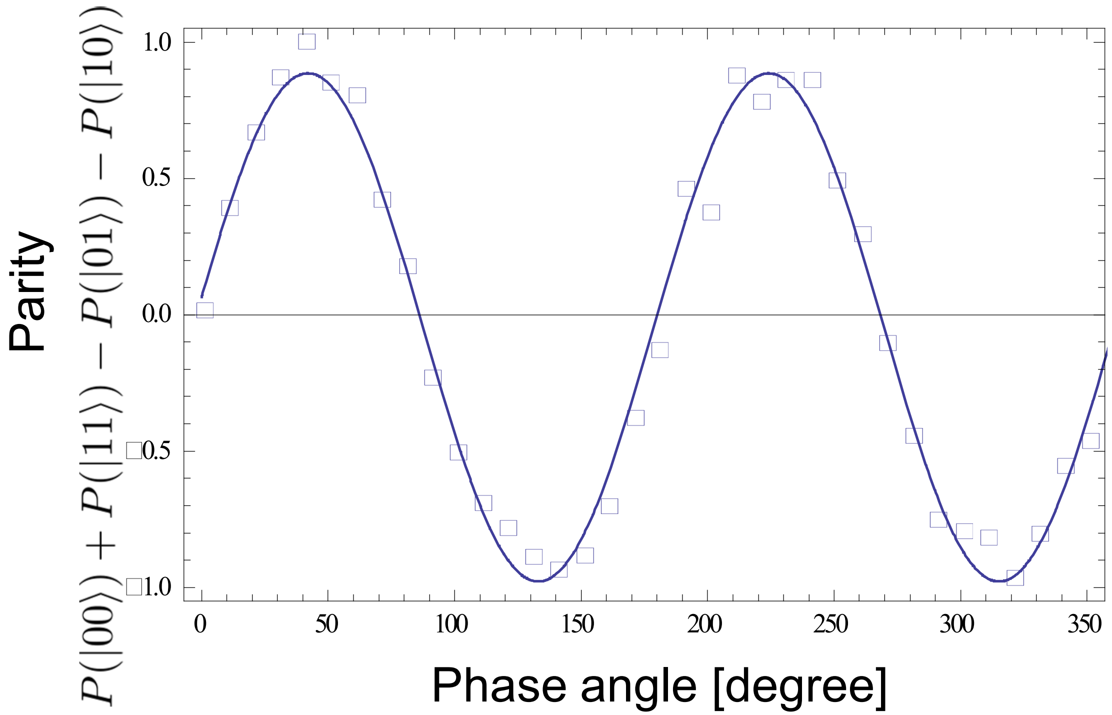

$$\mathcal{F} = \frac{1}{2}(P(|00\rangle) + P(|11\rangle)) + \frac{1}{4}c = 0.945$$

- Gate fidelity 94.5%
- Have yet to characterize sources of infidelity

Conclusion

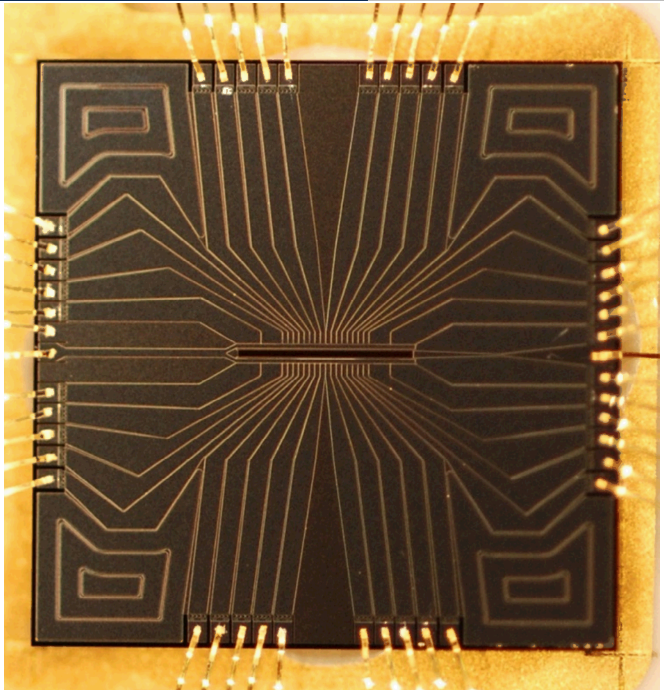

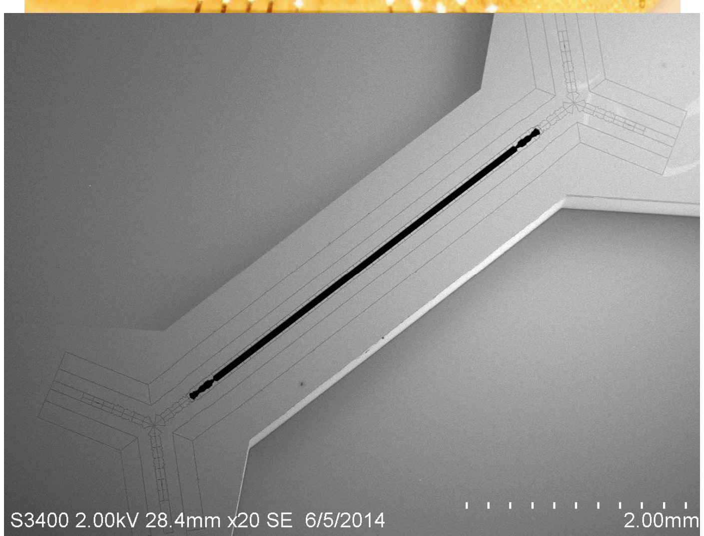

Microfabricated traps are ready for QIP

- Experiments were done in Thunderbird

Switching to HOA-2 brings advantages:

- Higher trap frequencies
- Optical access for individual addressing

Sandia National Laboratories

Thank you

State Detection using Histograms

Example histograms

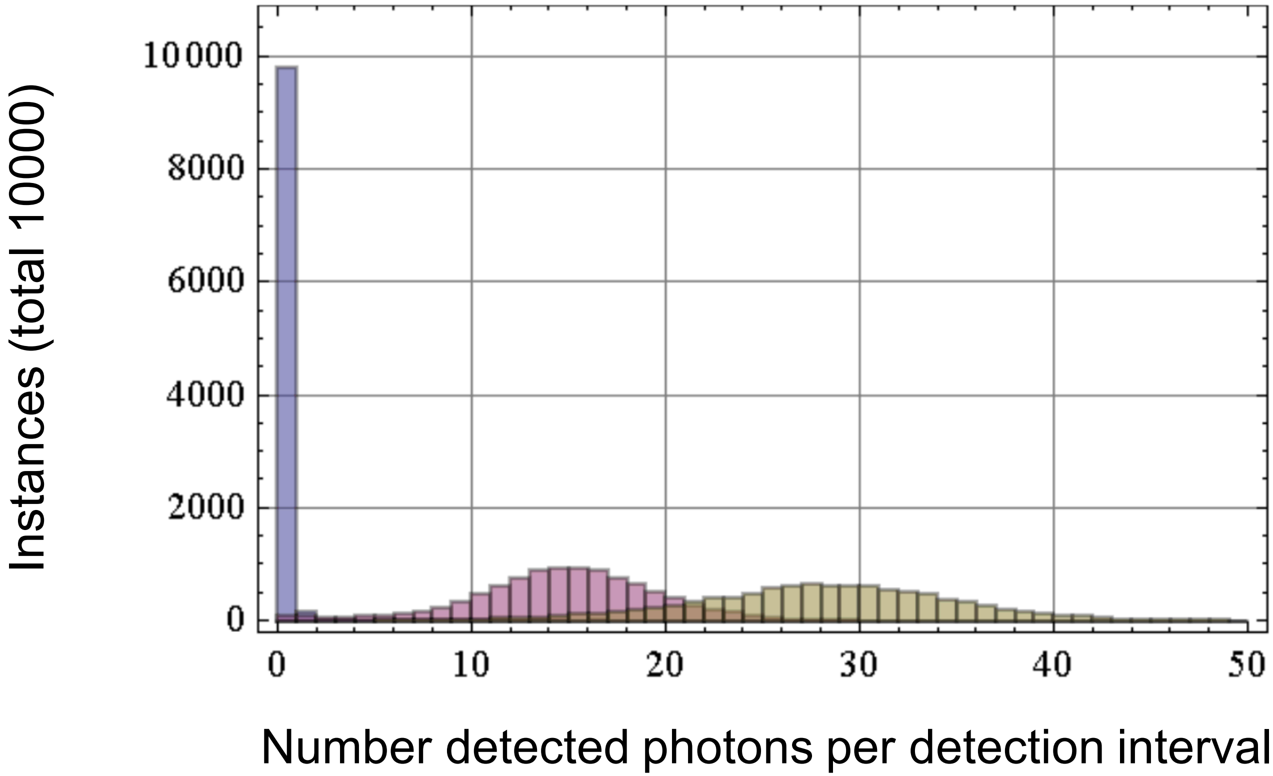

Long term plan: segmented PMT for individual state detection
Currently limited by optical crosstalk

State Detection Using Histograms

Global Rabi Oscillations on two ions

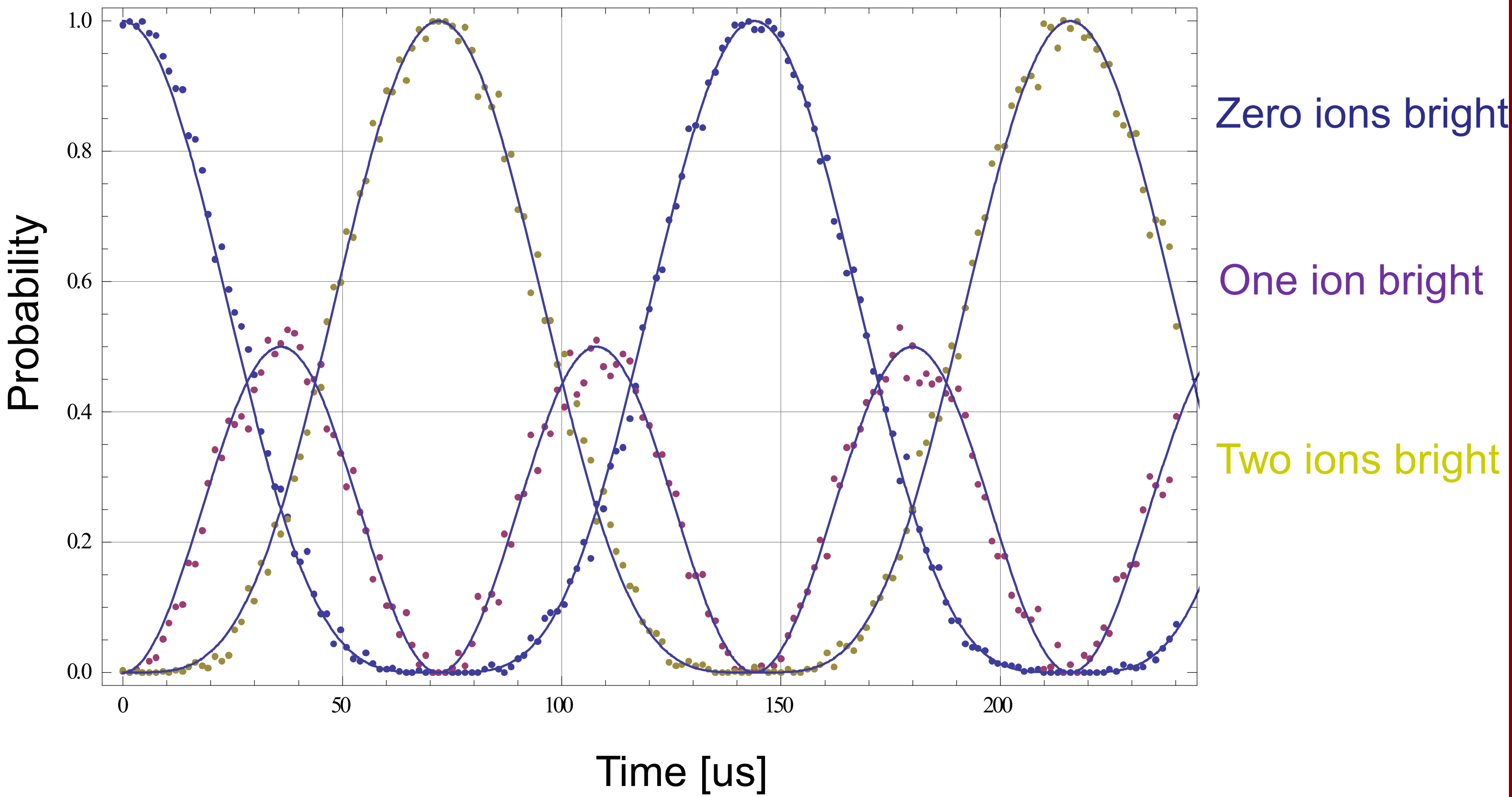

One parameter (Rabi time) is sufficient to simultaneously fit all three curves